coatings

Article

Coating Readily Available Yet Thermally Resistant Surfaces with 3D Silver Nanowire Scaffolds: A Step toward Efficient Heater Fabrication

Anas A. M. Alqanoo [1,2], Naser M. Ahmed [1,*], Md Roslan Hashim [1], Ahmed Alsadig [3], Shahad Al-Yousif [4], Sofyan A. Taya [2], Osamah A. Aldaghri [5] and Khalid Hassan Ibnaouf [5,*]

[1] School of Physics, Universiti Sains Malaysia, Penang 11800, Malaysia
[2] Physics Department, Islamic University of Gaza, Gaza P.O. Box 108, Palestine
[3] CNR NANOTEC Institute of Nanotechnology, Via Monteroni, 73100 Lecce, Italy
[4] Department of Electrical and Electronics Engineering, College of Engineering, Gulf University, Sanad 26489, Bahrain
[5] Physics Department, College of Science, Imam Mohammad Ibn Saud Islamic University (IMSIU), Riyadh 13318, Saudi Arabia
* Correspondence: naser@usm.my (N.M.A.); khiahmed@imamu.edu.sa (K.H.I.)

Abstract: In this study, we synthesized and characterized a 3D network of silver nanowires (AgNWs), employing the polyol approach in ethylene glycol (EG) as the reductant and polyvinylpyrrolidone (PVP) as the structure-directing agent for the growth of AgNWs to design inexpensive, timely responsive AgNWs-based heaters with different substrates. Data obtained from a field emission scanning electron microscope (FESEM) revealed that the average diameter of the synthesized AgNWs was 22 nm, and the average length was 28 µm. UV-visible absorption spectroscopy showed that AgNWs developed in a very pure phase. We investigated the impact of substrate type on the heating dissipation performance by depositing AgNW thin film over three chosen substrates made from readily available materials. The findings indicated that the AgNW-based heater with the wood substrate had the lowest response time of 21 s, the highest thermal resistance of 352.59 °C·cm^2/W, and a steady temperature of 135 °C at a low bias voltage of 5 V compared to cement (95 s, 297.77 °C·cm^2/W, and 120 °C) and glass (120 s, 270.25 °C·cm^2/W, and 110 °C).

Keywords: AgNWs; sheet resistance; heaters; absorption; wood; cement

check for updates

Citation: Alqanoo, A.A.M.; Ahmed, N.M.; Hashim, M.R.; Alsadig, A.; Al-Yousif, S.; Taya, S.A.; Aldaghri, O.A.; Ibnaouf, K.H. Coating Readily Available Yet Thermally Resistant Surfaces with 3D Silver Nanowire Scaffolds: A Step toward Efficient Heater Fabrication. *Coatings* **2023**, *13*, 315. https://doi.org/10.3390/coatings13020315

Academic Editor: Shijie Wang

Received: 26 December 2022
Revised: 17 January 2023
Accepted: 27 January 2023
Published: 31 January 2023

1. Introduction

Joule effect-based electrical heaters have garnered considerable interest due to their diverse uses, which include personal thermal management, defogging, defrosting, wearable devices, and industrial heating systems [1–4]. Mechanical properties, good thermal stability, fast response, as well as high heating temperature and low actuation voltage, are key parameters in evaluating the performance of electrical heaters [5,6]. Furthermore, electrical heaters that have a low sheet resistance R with a low applied voltage can produce sufficient Joule heat to raise the temperature of the film to a high saturation temperature [7].

Due to its high optical transmittance in the visible wavelength region and good electrical conductivity, indium tin oxide (ITO) has been widely employed to fabricate transparent film heaters. However, its inherent disadvantages, such as its delayed thermal response, costly ITO targets, instability in acids or bases, crack development under mechanical bending, and high-temperature fabrication process, are the main obstacles that limit the exploitation of the full potential of such materials [8,9]. Alternatively, graphene [10,11], metal grids, and carbon nanotubes [12,13] are regarded as potential alternatives for ITO with varying degrees of success [14,15]. However, in terms of optical transmittance and sheet resistance, these materials perform poorly when compared to ITO; thus, to employ them as efficient heaters, high voltage is required to obtain satisfactory heating outcomes [16].

Silver nanowires (AgNWs) have emerged as promising candidates to deposit conducting thin films [17]. An AgNW network exhibits mechanical compliance, high transparency, and excellent electrical and thermal conductivity [18–20]. Transparent electrodes based on AgNWs have been successfully used to fabricate several optoelectronic devices [21]. Transparent film heaters based on AgNWs have also been identified as viable candidates for the development of efficient and flexible film heaters [22]. In addition to the thin film's importance in producing high-performing heaters, the substrate type is also regarded as a key factor in producing quality heaters, since the substrate type can impact the heat dissipation, response time, and saturation temperature [23]. For instance, the relatively low thermal resistance of polyethylene terephthalate (PET) or polyethylene naphthalate (PEN) films limits the maximum temperature at which AgNW-based film heaters may reach. Furthermore, there is a weak bond between AgNW and the substrate; thus, the AgNW networks on the substrate are easily detachable and scratch-intolerant, which leads to poor conductivity and ineffective heat production [24]. Recently, it has been proposed that a thin layer of AgNW network embedded in the surface layer of a polymer substrate exhibits stronger binding between the AgNW and the substrate in transparent and flexible composite conductors [25]. As a result, the combination of a highly conductive AgNW network and a recently created polyacrylate-based heat-resistant polymer matrix serves as the inspiration for a revolutionary flexible and transparent film heater.

In order to enhance the response of the AgNWs heater with low bias voltage, an AgNW network was inserted in the surface of an in situ polymerized heat-resistant polymer film. The new polyacrylate-based heat-resistant polymer matrix was designed to give a set of required properties, including strong bonding with AgNWs, visual transparency, mechanical flexibility, and high glass transition temperature. The resulting conductive composite material exhibited a transmittance of 86.4% at 550 nm, a sheet resistance of 25 Ω sq^{-1}, and a high saturation temperature of up to 230 °C. The AgNW/SBS heaters based on nanocomposites, for instance, have a tensile strength of merely 1.2 MPa [26].

The employment of electrical heaters in high-performance heating systems in sectors such as the military and aerospace is severely constrained by their poor mechanical properties and thermal stability. To address this challenge, electrical heaters that are heat-resistant and mechanically robust are urgently required. Along this line, eco-friendly and readily accessible materials are highly demanded to substitute petroleum-based materials due to the rising demand of environmental conservation and energy [27]. Over thousands of decades, natural wood has been utilized extensively for buildings, furniture, and tools due to its high specific strength, simplicity of processing, high thermal resistivity, environmental friendliness, and broad availability [28–30]. Cement and wood are considered highly effective substrates and promising reinforcing phases. In addition, they are distinguished by their high thermal resistance, mechanical qualities, and specific heat [31].

In this work, high-purity AgNWs were produced by combining a novel purification technique with the salt mediator polyol approach. We developed three different heaters with various substrates, including wood, glass, and cement, using high-quality AgNWs with a high aspect ratio to explore the effect of the substrate on heater performance. The response time, heat dissipation, and thermal resistance were studied for each fabricated heater at five different bias voltages of 3, 3.5, 4, 4.5, and 5 V. This study may open a wide field for fabricating a highly transparent and flexible heater based on transparent wood.

2. Materials and Methods

2.1. Materials

Silver nitrates ($AgNO_3$), polyvinyl pyrrolidone (PVP-1300000), sodium chloride (NaCl), and potassium bromide (KBr) were purchased from Sigma Aldrich company (Sigma-Aldrich (M) Sdn. Bhd., Penang, Malaysia). Ethanol (99.5%), acetone (99%), and ethylene glycol (EG) were purchased from the chemical store in Universiti Sains (Penang, Malaysia). All experiments needed deionized (DI) water that was obtained by a Direct-Q 5. The ultraviolet (UV) water purification system had a resistivity of 18.5 MΩ·cm.

2.2. Synthesis and Characterization of AgNWs

AgNWs were fabricated using a polyol process, as reported in our previous work, with some modifications [13]. As depicted in Figure 1a, solutions of PVP (330 mg in 8 mL of EG), NaCl (80 mg in 8 mL of EG), KBr (170 mg in 8 mL of EG), and $AgNO_3$ (170 mg in 10 mL of EG) were prepared. In Figure 1b, 8 mL of EG was injected into a 50 mL flask and put in an oil bath at a temperature of 155 °C under stirring of 200 rpm for 15 min. Then, 80 µL of KBr, 130 µL of NaCl, and 8 mL of PVP solutions were pipetted into the flask and kept at the same temperature for another 15 min with continuous stirring. Next, 10 mL of $AgNO_3$ was slowly injected using a syringe pump into the solution for 10 min. The reacting mixture was left until the colour became greenish-gray. Following that, DI water was added to the solution at a 1:1 ratio and was allowed to cool down to room temperature. Figure 1c shows the purification process. Due to the presence of heavy particles and nanorods in the solution, a centrifugation of 1500 rpm was utilized to precipitate them. The supernatant contained the ultra-light silver nanowires. The solution was diluted by acetone three times separately and then re-washed three times by ethanol, and the final AgNWs were redispersed in 10 mL of ethanol. The structural morphology of the AgNW-based heaters was obtained using field emission scanning electron microscopy operated at 5 kV (FESEM, Carl Zeiss, SUPRA 40VP, OPTO-EDU, Wanda Plaza, Changchun, China). The crystallinity of AgNWs was measured using X-ray diffraction analysis (XRD, D8 Advance X-ray diffractometer, Bruker, Billerica, MA, USA, Cu K irradiation at = 1.54060 Å). A transmission electron microscope (TEM, Libra 120, Universiti Sains Malaysia, Penang, Malaysia) operating at 120 kV was used to investigate the morphologies of the colloidal AgNWs. The Agilent Carry 5000 absorption spectrophotometer was employed to obtain the optical profile using the UV-Vis (PerkinElmer, with λ = 952 nm, Waltham, MA, USA) absorption spectra of the AgNW suspension.

2.3. Deposition of AgNWs Heaters Based on Different Substrates

As illustrated in Figure 2, a very thin AgNW layer through the spray coating process was formed on top of three different substrates, glass, concrete, and wood (Oak), with the same square area of 6.25 cm^2 and same thickness of 2 mm. All of the substrates were sprayed under the same conditions, with a spraying time of 5 s and a distance of 10 cm between each substrate and the spray gun. The morphology of the deposition layer was analysed with electron microscopes (FESEM, and TEM). An infrared thermometer with a model of (Fluke 62 MAX. IR thermometer, Everett, WA, USA) was used to determine the temperature of the AgNW network.

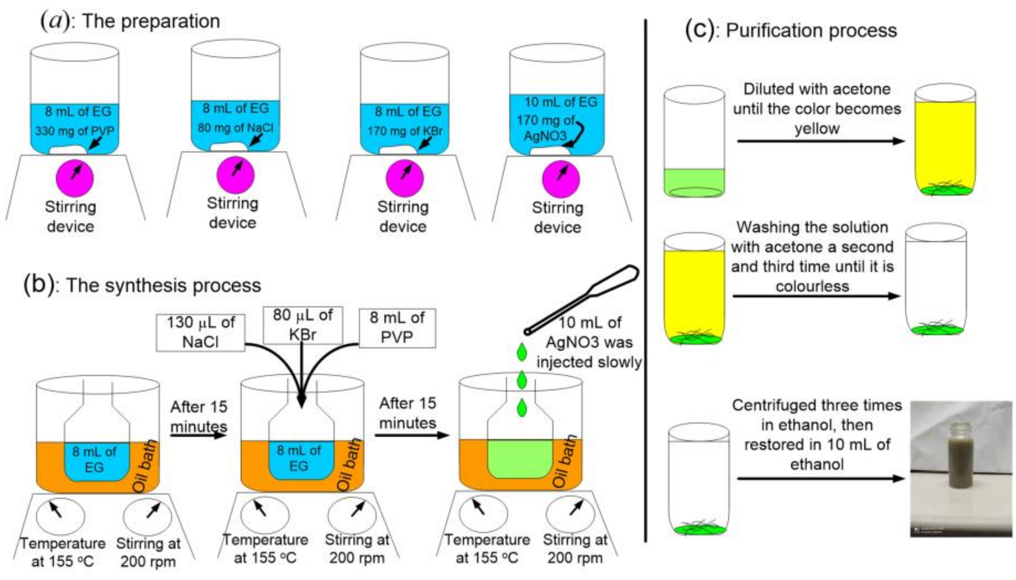

Figure 1. Schematic diagram illustrating (**a**) the preparation of precursor solutions; (**b**) synthesis protocol using the modified polyol method; and (**c**) the purification strategy used for the AgNW fabrication.

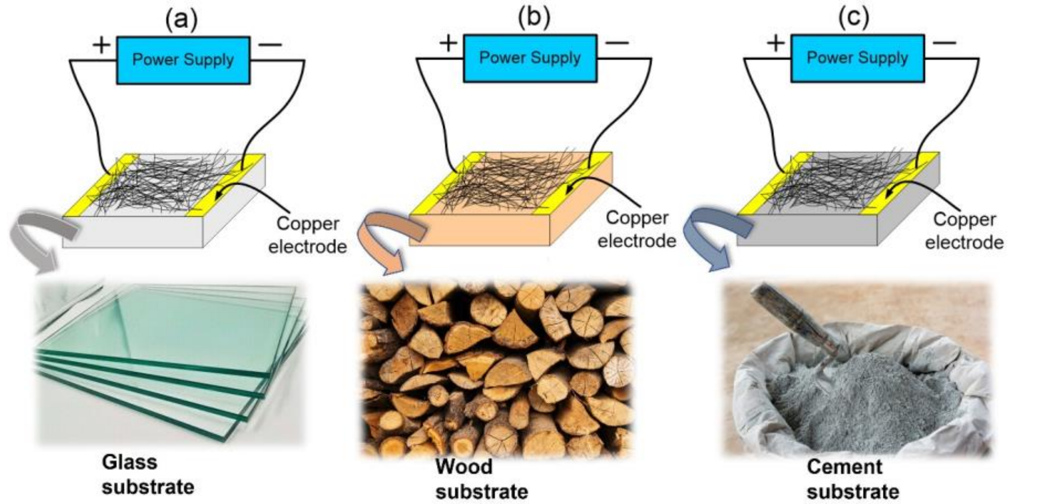

Figure 2. A cartoon illustrating the structure of the heater devices fabricated with (**a**) AgNWs/glass; (**b**) AgNWs/wood; and (**c**) AgNWs/cement.

3. Results and Discussion

3.1. Characterization of the Obtained AgNWs

The surface morphology of the highly-purified AgNWs was studied using FESEM and TEM as shown in Figure 3. As can be seen from the figure, the 1D structures were found to be highly uniform, to contain no by-products, and to have a measured aspect ratio of 1272. Moreover, the TEM image (Figure 3b) demonstrates the considerable regularity, which may be useful for the heater based on AgNWs.

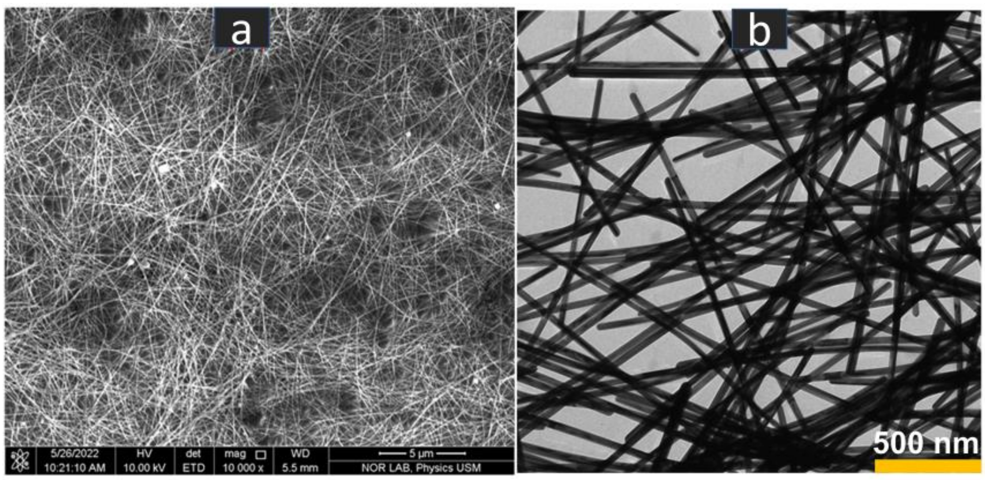

Figure 3. Electron micrograph showing (**a**) FESEM and (**b**) TEM images of AgNWs prepared using the modified polyol technique.

The optical absorption spectrum of the redispersed AgNWs was recorded using a UV–Visible-IR spectrophotometer as shown in Figure 4. Two prominent peaks were found at wavelengths of 370 and 353 nm, which correspond to the transverse and longitudinal surface plasmonic resonance of silver nanostructures, respectively. Moreover, at the 371 nm peak, the low half width indicated the negligible by-products and the purity of the prepared solution, which was consistent with the electron micrographs shown in Figure 3. These findings highlight the ability of producing ultra-light AgNWs, which allows for reducing the number of wire-wire junctions and the sheet resistance of the film to achieve our objective of fabricating AgNW network-based efficient heater devices at a low operation voltage. The XRD analysis of manufactured AgNWs coated on a glass substrate is shown in Figure 5. JCPDF87-0710 [32,33] attributes the cubic structures of {111} and {200} of metallic

Ag to the diffraction peaks that are positioned at 2θ of 38.12° and 44.2°. The high pure crystallinity of the synthesized AgNWs was confirmed by the substantial intensity ratio between the {111} peak and the {200} peak, which also showed that wires develop rapidly in the {111} direction to produce ultra-thin AgNWs. These results agree with those mentioned in the literature [34,35]. Figure 6 shows FESEM images of AgNW thin film sprayed over the surface of the selected substrates. As clearly seen in the figure, the high roughness of the cement and wood compared to the glass may enhance the adhesion of AgNWs to their surfaces.

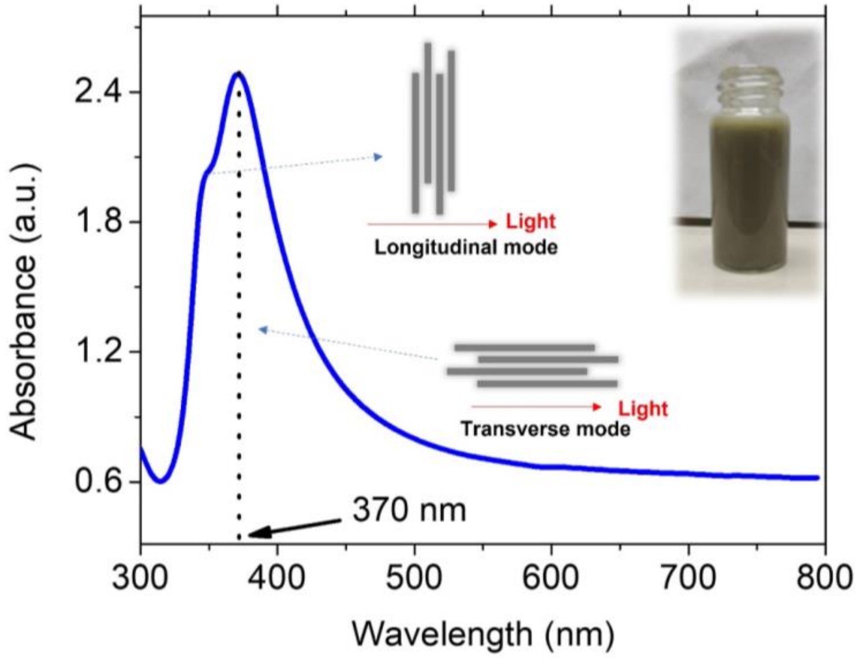

Figure 4. The UV-Visible spectrum of the silver nanowires that were suspended in ethanol and synthesized utilizing the salt mediator polyol method.

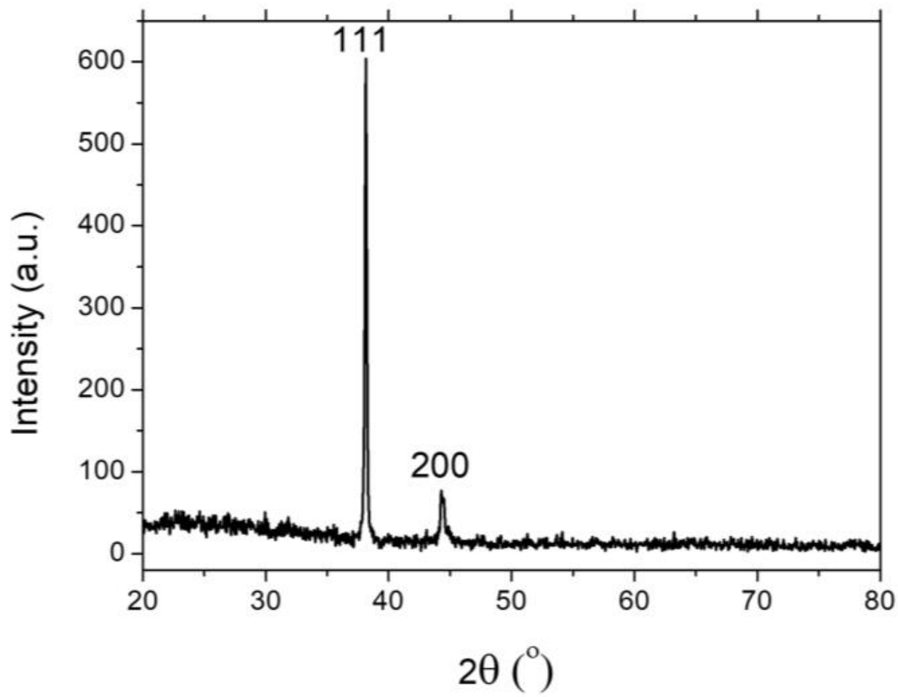

Figure 5. XRD patterns of the produced AgNWs.

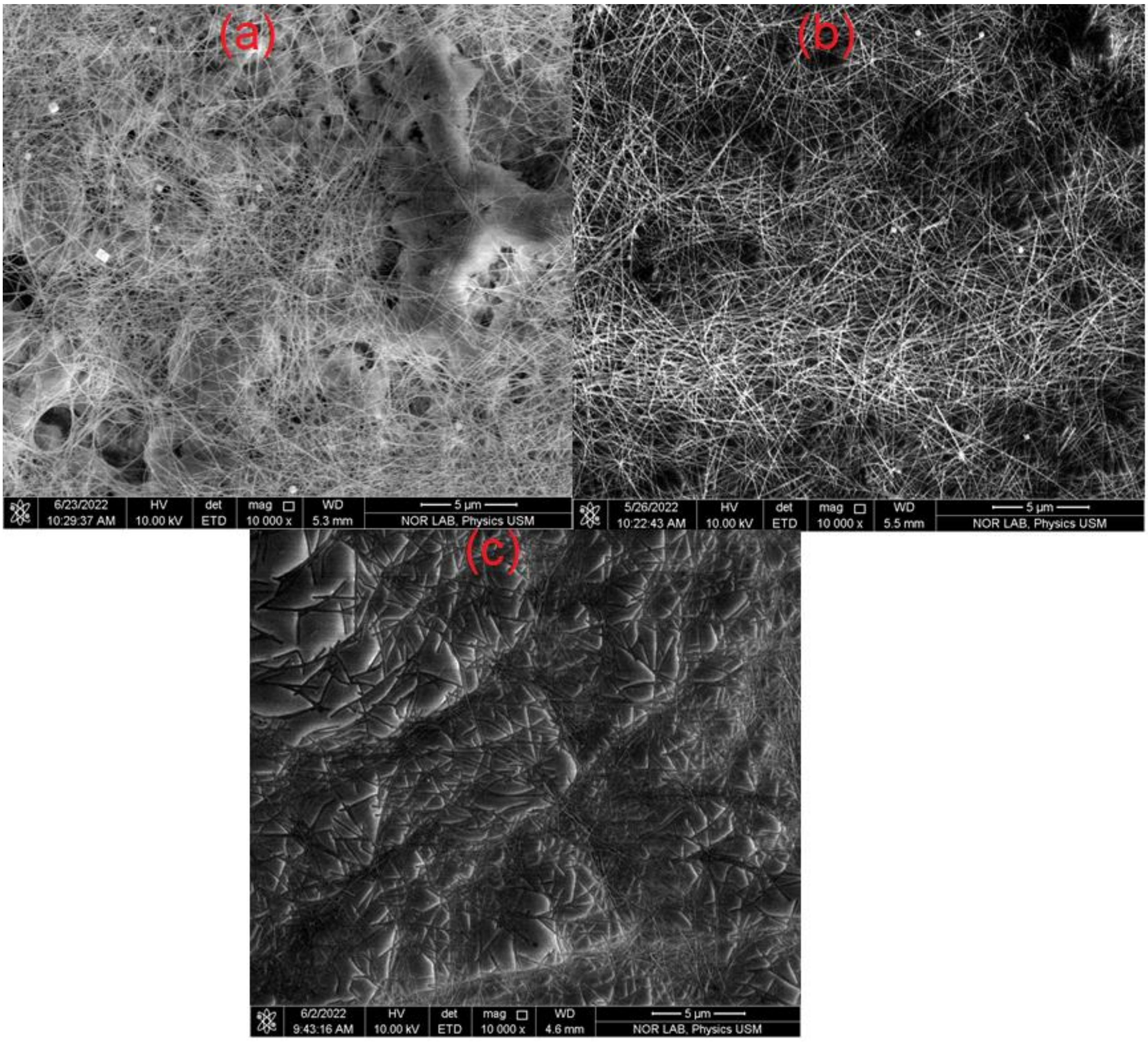

Figure 6. FESEM images of (**a**) AgNWs/cement; (**b**) AgNWs/wood; and (**c**) AgNWs/glass.

3.2. Characterization of AgNW-Based Heaters: Temperature-Time Analysis

In order to understand the working mechanism of the heaters based on AgNWs, the relationship among the steady temperature, the response time, and the dissipation heat was derived. Firstly, electrical energy Q_e was supplied to the AgNW film using Joule's law, which is defined as:

$$Q_e = \frac{V^2}{R} t \tag{1}$$

where V is the supplied voltage, R is the sheet resistance of the film, and t is the response time, which is defined as the time interval that passes before it reaches saturation temperature. After supplying the electric voltage, the electrical energy starts to be converted to heat energy (Q_f) in the AgNW film, which is considered the heat source in our implementation. However, this energy is dissipated in the substrate, which is known as dissipation energy (Q_d), considering that the heat dissipation through radiation should be neglected at temperatures less than 140 °C. Therefore, selecting the type of substrate is crucial in fabricating AgNW-based heaters. For an AgNW film of mass (m) and specific heat (c), the electric power raises the temperature from room temperature (T_r) to steady temperature (T_s), with heat energy (Q_f) given by the following equation:

$$Q_f = m\, c\, (T_s - T_r) \tag{2}$$

Due to the conservative energy law, the formula that relates the electric energy, heat energy in the film, and the dissipation energy is written as:

$$Q_e = Q_f + Q_d \tag{3}$$

Equations (1)–(3) are then solved for T_s, which is written as:

$$T_s = \frac{\frac{V^2}{R}\, t - Q_d}{m\, c} + T_r \tag{4}$$

The parameters used in evaluating the performance of the AgNW heaters are steady temperature, bias voltages, response time, and thermal resistance, which mainly depends on the dissipation heat and, therefore, on the type of substrate. Three heaters with the same sheet resistance of 10 Ω/sq were fabricated by coating an AgNW solution on three substrates: glass, wood, and cement. Over the coating surface with an area of 2.5 cm × 2.5 cm, AgNWs were evenly dispersed and randomly oriented. The transient responses of the three fabricated heaters with the three different substrates driven at five input voltages of 3, 3.5, 4, 4.5, and 5 V are shown in Figure 7. Once the thermal balancing between the heat energy of the AgNW film and the dissipation energy through the substrate was attained, the temperature reached steady state.

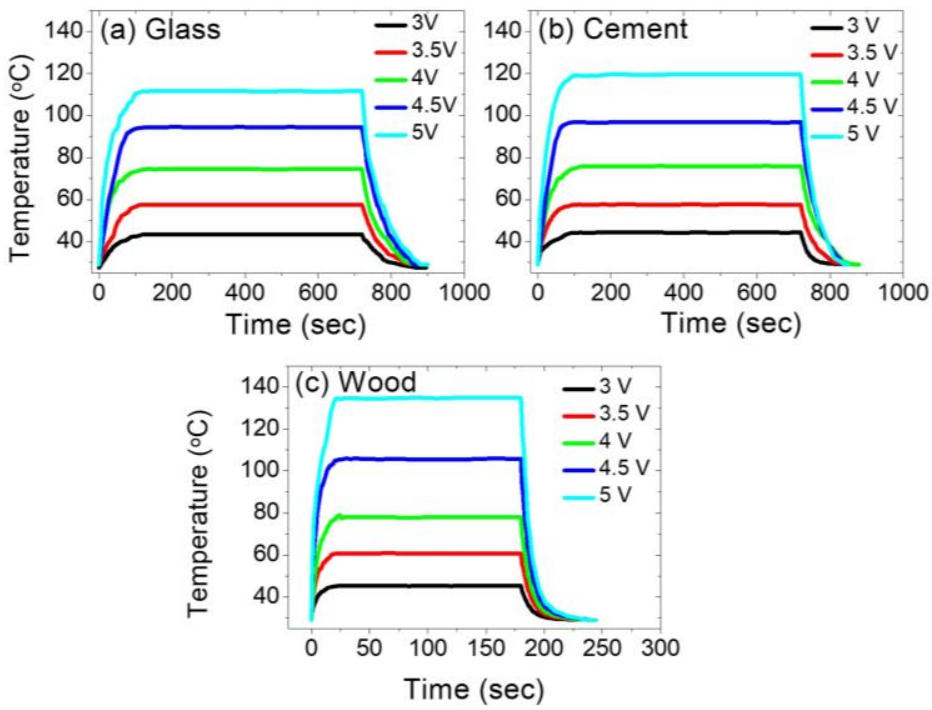

Figure 7. Temperature response versus time of (**a**) AgNWs/glass; (**b**) AgNWs/cement; and (**c**) AgNWs/wood heaters, respectively, at five bias voltages: 3, 3.5, 4, 4.5, and 5 V.

As shown in Figure 7a, the AgNW heater based on the glass substrate with a bias voltage of 5 V reached a steady temperature of 112 °C, while the saturation temperatures at bias voltages of 4.5, 4, 3.5, and 3 V were 94.5, 74.6, 57, and 43 °C, respectively. Figure 7b shows that the steady temperatures of the cement heater-based AgNWs are 120, 97, 76, 57.8, and 44 °C at bias voltages of 5, 4.5, 4, 3.5, and 3 V, respectively. A sample of an

AgNW-coated substrate measurement is displayed in Scheme S1. It was observed from Figure 7c that the steady temperature at the voltage 5 V was 135 °C for the wood substrate, which is considered a decent result at the low operating voltage (5 V), thanks to the high thermal resistance of the wood, compared to the other materials that were previously reported [1,36–38]. The steady temperatures at the other voltages, 4.5, 4, 3.5, and 3 V, of the wood heater were 106, 79, 60.8, and 45.4 °C, respectively. It is clear from Equation (4) that response time (t) and steady temperature (T_s) are functions of Q_d that depend mainly on substrate type. Herein, because of the high thermal resistance [39] and high specific heat of wood compared to glass and cement, the dissipation energy (Q_d) was very low, and as a result, the response time in the wood case was very low (21 s), while a rapid growth of temperature was achieved compared to the cement substrate (95 s) and the glass substrate (121 s), regardless of the applied voltage as shown in Figure 7. This means that AgNW functionalized wood substrates reached a high temperature in a short time interval. The possibility of reaching 135 °C in 21 s at 5 V is considered an interesting outcome, bearing in mind the high thermal resistance compared to cement and glass. On the other hand, in a comparison between cement and glass heaters, the heat dissipation was found to be less in cement than glass due to its higher thermal resistance and higher specific heat; therefore, the cement heater displayed a rapid temperature response. In contrast to the cement-based heaters, AgNW wood-based heaters showed remarkable performance.

3.3. Temperature-Input Power Density Analysis

Thermal resistance is considered a key factor in evaluating a heater's performance. Figure 8 displays our analysis of the steady temperatures versus the supplied power density (power per unit area) for the substrates employed in this work. The three heaters exhibited the same steady temperatures at low power densities until 0.18 W/cm^2. This finding further demonstrates the superiority of the film heaters based on wood substrates. Using the slope of the fitted line depicting the steady temperature versus input power density in Figure 8a, the thermal resistance was determined for AgNWs/glass, AgNWs/cement, and AgNWs/wood heaters. Figure 8b displays the results of comparing the three heaters in terms of their thermal resistance. While the AgNWs/cement heater had a thermal resistance of 297.77 °C·cm^2·W^{-1}, which is around 10.18% greater than the AgNWs/glass heater's thermal resistance (270.25 °C·cm^2·W^{-1}), the AgNWs/wood heater had 352.59 °C·cm^2·W^{-1}, about 30.46% and 18.41% greater than the AgNWs/glass and AgNWs/cement heaters, respectively. Table 1 compares the response time, steady temperature, and thermal resistance of AgNWs/glass, AgNWs/cement, and AgNWs/wood heaters with other previous studies. The results show that the AgNWs heaters with the wood substrate have a much higher power efficiency than the cement and glass substrates. Based on the findings of the heating performance evaluation, the AgNW/wood heater was proven to be an effective replacement for traditional film heaters.

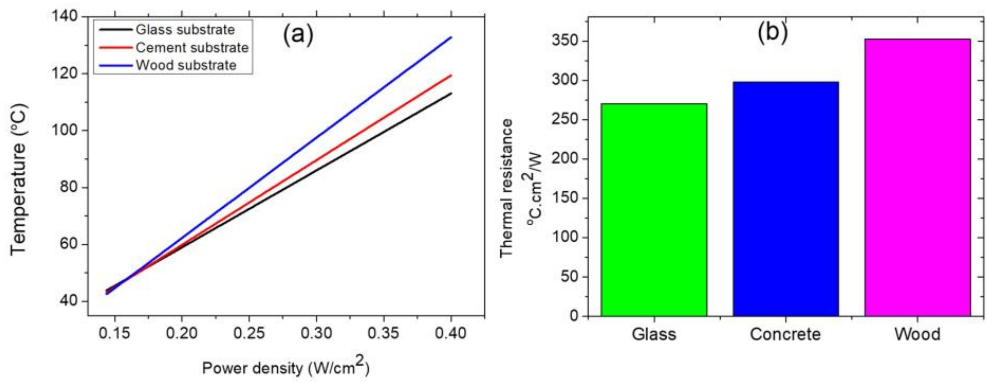

Figure 8. (**a**) Steady temperature versus the input power density for AgNWs/glass, AgNWs/cement, and AgNWs/wood heaters; and (**b**) s comparison between the thermal resistance per unit area of the three heaters.

Table 1. Comparison between the current study and the literature for the important parameters of heaters based on AgNWs.

Heater	Voltage (V)	Response Time (s)	Steady Temperature (°C)	Thermal Resistance °C·cm^2/w	Reference
AgNW-PEDOT: PSS/ITO	5	70	43	210.3	[36]
AgNW/polyimide	5	40	76	160.6	[37]
AgNWs/polyacrylate	5	40	81	-	[38]
AgNWs/PEDOT: PSS	5	25	74.5	-	[1]
AgNWs/glass	5	121	112	270.25	Current study
AgNWs/cement	5	95	120	297.77	Current study
AgNWs/wood	5	21	135	352.59	Current study

3.4. Temperature-Voltage Characteristics

To better evaluate the heater performance, for the first time, the uncertainty of the steady temperature with respect to the uncertainty of the bias voltage (δT/δV) was proposed, which determines the sensitivity of the heater to the temperature due to the small change in bias voltage. The uncertainty here was calculated directly from the T-V curve using the origin software. Figure 9 shows the steady temperature versus the bias voltage within three AgNW heaters by Joule heating. It is clear from the figure that the uncertainty of the AgNWs/wood heater was significantly higher than the other heaters. For instance, at a 5 V-bias voltage, AgNWs/wood had an uncertainty 31.5% higher than the uncertainty of AgNWs/cement and 65.7% higher than the uncertainty of AgNW/glass. These results are consistent with the other findings demonstrated in previous sections.

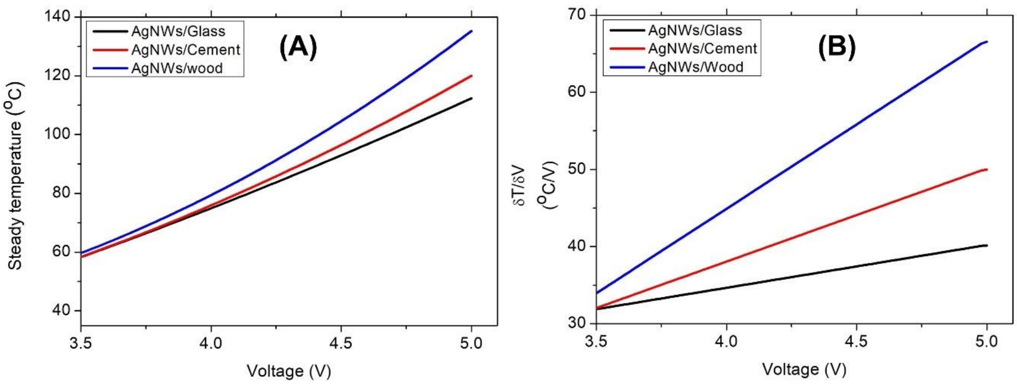

Figure 9. (**A**) The steady temperature via the bias voltage of the three heaters, and (**B**) the uncertainty of the steady temperature with respect to the uncertainty of the bias voltage.

4. Conclusions

In this study, a series of ultra-thin AgNWs were obtained and highly purified using an optimized purification approach. NaCl and KBr were introduced to the fabrication procedure to regulate the concentration of free Ag+ ions. Based on FESEM findings, AgNWs with a diameter of 22 nm and a length of 28 µm were produced. The AgNW UV-Visible spectrum with a sharp peak confirmed that AgNWs were synthesized in a highly pure condition. These AgNWs were utilized to produce a low-cost, high-efficiency heater composed of AgNWs and wood. At a 5 V-bias voltage, the fabricated AgNWs/wood heater had a steady temperature of 135 °C, a response time of 21 s, and a thermal resistance of 352.59 °C·cm^2/W. The uncertainty δT/δV for the AgNWs/wood heater had a high value of 66.5 °C/V relative to the AgNWs/cement and AgNWs/glass heaters, with uncertainties of 50.56 °C/V and 40.14 °C/V, respectively. The superior performance of the wood is attributed to its high thermal resistance, high specific heat, and, as a result, the low dissipation of heat through the wood substrate. With further investigations, the wood substrates might be improved, and these substrates could be employed to produce high-performance, flexible, transparent heaters.

Supplementary Materials: The following supporting information can be downloaded at: https://www.mdpi.com/article/10.3390/coatings13020315/s1, Scheme S1: Real images during the measurement process.

Author Contributions: Conceptualization, S.A.T. and N.M.A.; methodology, A.A.M.A. and A.A.; software, N.M.A. and M.R.H.; validation, K.H.I. and M.R.H.; formal analysis, A.A.M.A. and A.A.; investigation, A.A.M.A.; resources, K.H.I.; data curation, N.M.A.; writing—original draft preparation, A.A.M.A.; writing—review and editing, S.A.-Y., S.A.T., A.A. and O.A.A.; visualization, S.A.-Y. and O.A.A.; supervision, N.M.A. and M.R.H.; project administration, K.H.I. and N.M.A.; funding acquisition, K.H.I. All authors have read and agreed to the published version of the manuscript.

Funding: The authors extend their appreciation to the Deanship of Scientific Research at Imam Mohammad Ibn Saud Islamic University (IMSIU) for funding and supporting this work through Research Partnership Program no. RP-21-09-41.

Institutional Review Board Statement: Not applicable.

Informed Consent Statement: Not applicable.

Data Availability Statement: Not applicable.

Acknowledgments: The authors are thankful to the Deanship of Scientific Research at Imam Mohammad Ibn Saud Islamic University (IMSIU) for supporting this work.

Conflicts of Interest: The authors declare no conflict of interest.

References

1. Zhang, M.; Wang, C.; Liang, X.; Yin, Z.; Xia, K.; Wang, H.; Jian, M.; Zhang, Y. Weft-knitted fabric for a highly stretchable and low-voltage wearable heater. *Adv. Electron. Mater.* **2017**, *3*, 1700193. [CrossRef]
2. Jang, N.S.; Kim, K.H.; Ha, S.H.; Jung, S.H.; Lee, H.M.; Kim, J.M. Simple approach to high-performance stretchable heaters based on kirigami patterning of conductive paper for wearable thermotherapy applications. *ACS Appl. Mater. Interfaces* **2017**, *9*, 19612–19621. [CrossRef] [PubMed]
3. Yao, Y.; Fu, K.K.; Yan, C.; Dai, J.; Chen, Y.; Wang, Y.; Zhang, B.; Hitz, E.; Hu, L. Three-dimensional printable high-temperature and high-rate heaters. *ACS Nano* **2016**, *10*, 5272–5279. [CrossRef] [PubMed]
4. Tian, S.; He, P.; Chen, L.; Wang, H.; Ding, G.; Xie, X. Electrochemical fabrication of high quality graphene in mixed electrolyte for ultrafast electrothermal heater. *Chem. Mater.* **2017**, *29*, 6214–6219. [CrossRef]
5. An, B.W.; Gwak, E.J.; Kim, K.; Kim, Y.C.; Jang, J.; Kim, J.Y.; Park, J.U. Stretchable, transparent electrodes as wearable heaters using nanotrough networks of metallic glasses with superior mechanical properties and thermal stability. *Nano Lett.* **2016**, *16*, 471–478. [CrossRef] [PubMed]
6. Wang, R.; Xu, Z.; Zhuang, J.; Liu, Z.; Peng, L.; Li, Z.; Liu, Y.; Gao, W.; Gao, C. Highly stretchable graphene fibers with ultrafast electrothermal response for low-voltage wearable heaters. *Adv. Electron. Mater.* **2017**, *3*, 1600425. [CrossRef]
7. Li, P.; Ma, J.; Xu, H.; Xue, X.; Liu, Y. Highly stable copper wire/alumina/polyimide composite films for stretchable and transparent heaters. *J. Mater. Chem. C* **2016**, *4*, 3581–3591. [CrossRef]
8. Zheng, B.; Zhu, Q.; Zhao, Y. Fabrication of high-quality silver nanowire conductive film and its application for transparent film heaters. *J. Mater. Sci. Technol.* **2021**, *71*, 221–227. [CrossRef]
9. Sui, D.; Huang, Y.; Huang, L.; Liang, J.; Ma, Y.; Chen, Y. Flexible and transparent electrothermal film heaters based on graphene materials. *Small* **2011**, *7*, 3186–3192. [CrossRef]
10. Xu, Z.; Liu, Z.; Sun, H.; Gao, C. Highly electrically conductive Ag-doped graphene fibers as stretchable conductors. *Adv. Mater.* **2013**, *25*, 3249–3253. [CrossRef]
11. Liu, P.; Liu, L.; Jiang, K.; Fan, S. Carbon-nanotube-film microheater on a polyethylene terephthalate substrate and its application in thermochromic displays. *Small* **2011**, *7*, 732–736. [CrossRef]
12. Kim, D.; Lee, H.-C.; Woo, J.Y.; Han, C.-S. Thermal behavior of transparent film heaters made of single-walled carbon nanotubes. *J. Phys. Chem. C* **2010**, *114*, 5817–5821. [CrossRef]
13. Wu, Z.P.; Wang, J.N. Preparation of large-area double-walled carbon nanotube films and application as film heater. *Phys. E Low-Dimens. Syst. Nanostruct.* **2009**, *42*, 77–81. [CrossRef]
14. Kumar, A.; Zhou, C. The race to replace tin-doped indium oxide: Which material will win? *ACS Nano* **2010**, *4*, 11–14. [CrossRef] [PubMed]
15. Hecht, D.S.; Hu, L.; Irvin, G. Emerging transparent electrodes based on thin films of carbon nanotubes, graphene, and metallic nanostructures. *Adv. Mater.* **2011**, *23*, 1482–1513. [CrossRef] [PubMed]
16. Madaria, A.R.; Kumar, A.; Zhou, C. Large scale, highly conductive and patterned transparent films of silver nanowires on arbitrary substrates and their application in touch screens. *Nanotechnology* **2011**, *22*, 245201. [CrossRef] [PubMed]

17. Langley, D.; Giusti, G.; Mayousse, C.; Celle, C.; Bellet, D.; Simonato, J.-P. Flexible transparent conductive materials based on silver nanowire networks: A review. *Nanotechnology* **2013**, *24*, 452001. [CrossRef] [PubMed]
18. Kim, A.; Won, Y.; Woo, K.; Kim, C.-H.; Moon, J. Highly transparent low resistance ZnO/Ag nanowire/ZnO composite electrode for thin film solar cells. *ACS Nano* **2013**, *7*, 1081–1091. [CrossRef]
19. Alqanoo, A.A.; Ahmed, N.M.; Hashim, N.R.; Almessiere, M.A.; Taya, S.A.; Zyoud, S.H. Silver nanowires assisted porous silicon for high photodetector sensitivity using surface plasmonic phenomena. *Sens. Actuators A Phys.* **2022**, *347*, 113942. [CrossRef]
20. Alqanoo, A.A.M.; Ahmed, N.M.; Hashim, M.R.; Almessiere, M.A.; Taya, S.A.; Alsadig, A.; Aldaghri, O.A.; Ibnaouf, K.H. Synthesis and deposition of silver nanowires on porous silicon as an ultraviolet light photodetector. *Nanomaterials* **2023**, *13*, 353. [CrossRef]
21. Liao, Q.; Hou, W.; Zhang, J.; Qin, L. Controllable preparation of silver nanowires and its application in flexible stretchable electrode. *Coatings* **2022**, *12*, 1756. [CrossRef]
22. You, J.; Lee, S.M.; Eom, H.S.; Chang, S.T. Highly transparent conducting electrodes based on a grid structure of silver nanowires. *Coatings* **2020**, *11*, 30. [CrossRef]
23. Wu, X.; Zhou, Z.; Wang, Y.; Li, J. Syntheses of silver nanowires ink and printable flexible transparent conductive film: A review. *Coatings* **2020**, *10*, 865. [CrossRef]
24. Hong, S.; Yeo, J.; Kim, G.; Kim, D.; Lee, H.; Kwon, J.; Lee, H.; Lee, P.; Ko, S.H. Nonvacuum, maskless fabrication of a flexible metal grid transparent conductor by low-temperature selective laser sintering of nanoparticle ink. *ACS Nano* **2013**, *7*, 5024–5031. [CrossRef] [PubMed]
25. Hu, W.; Niu, X.; Zhao, R.; Pei, Q. Elastomeric transparent capacitive sensors based on an interpenetrating composite of silver nanowires and polyurethane. *Appl. Phys. Lett.* **2013**, *102*, 38. [CrossRef]
26. Song, C.; Hwang, H.J.; Kim, J.H.; Hyeon, T.; Kim, D.H. Stretchable heater using ligand-exchanged silver nanowire nanocomposite for wearable articular thermotherapy. *ACS Nano* **2015**, *9*, 6626–6633.
27. Mao, Y.; Hu, L.; Ren, Z.J. Engineered wood for a sustainable future. *Matter* **2022**, *5*, 1326–1329. [CrossRef]
28. Toumpanaki, E.; Shah, D.U.; Eichhorn, S.J. Beyond what meets the eye: Imaging and imagining wood mechanical-structural properties. *Adv. Mater.* **2021**, *33*, 2001613. [CrossRef]
29. Liu, C.; Luan, P.C.; Li, Q.; Cheng, Z.; Xiang, P.Y.; Liu, D.T.; Hou, Y.; Yang, Y.; Zhu, H. Biopolymers derived from trees as sustainable multifunctional materials: A review. *Adv. Mater.* **2020**, *33*, 2001654. [CrossRef]
30. Ajdary, R.; Tardy, B.L.; Mattos, B.D.; Bai, L.; Rojas, O.J. Plant nanomaterials and inspiration from nature: Water interactions and hierarchically structured hydrogels. *Adv. Mater.* **2020**, *33*, 2001085. [CrossRef]
31. Huang, J.L.; Zhao, B.; Liu, T.; Mou, J.; Jiang, Z.J.; Liu, J.; Li, H.; Liu, M. Wood-derived materials for advanced electrochemical energy storage devices. *Adv. Funct. Mater.* **2019**, *29*, 1902255. [CrossRef]
32. Cakici, M.; Kakarla, R.R.; Alonso-Marroquin, F. Advanced electrochemical energy storage supercapacitors based on the flexible carbon fiber fabric-coated with uniform coral-like MnO2 structured electrodes. *Chem. Eng. J.* **2017**, *309*, 151–158. [CrossRef]
33. Sauer, G.; Brehm, G.; Schneider, S.; Nielsch, K.; Wehrspohn, R.B.; Choi, J.; Hofmeister, H.; Gösele, U. Highly ordered monocrystalline silver nanowire arrays. *J. Appl. Phys.* **2002**, *91*, 3243–3247. [CrossRef]
34. Zhang, D.; Qi, L.; Yang, J.; Ma, J.; Cheng, H.; Huang, L. Wet chemical synthesis of silver nanowire thin films at ambient temperature. *Chem. Mater.* **2004**, *16*, 872–876. [CrossRef]
35. Coskun, S.; Aksoy, B.; Unalan, H.E. Polyol synthesis of silver nanowires: An extensive parametric study. *Cryst. Growth Des.* **2011**, *11*, 4963–4969. [CrossRef]
36. Park, J.; Han, D.; Choi, S.; Kim, Y.; Kwak, J. Flexible transparent film heaters using a ternary composite of silver nanowire, conducting polymer, and conductive oxide. *RSC Adv.* **2019**, *9*, 5731–5737. [CrossRef] [PubMed]
37. Huang, Q.; Shen, W.; Fang, X.; Chen, G.; Guo, J.; Xu, W.; Tan, R.; Song, W. Highly flexible and transparent film heaters based on polyimide films embedded with silver nanowires. *RSC Adv.* **2015**, *5*, 45836–45842. [CrossRef]
38. Li, J.; Liang, J.; Jian, X.; Hu, W.; Li, J.; Pei, Q. A flexible and transparent thin film heater based on a silver nanowire/heat-resistant polymer composite. *Macromol. Mater. Eng.* **2014**, *299*, 1403–1409. [CrossRef]
39. Tsapko, Y.; Tsapko, A.; Bondarenko, O. Determination of the laws of thermal resistance of wood in application of fire-retardant fabric coatings. *East.-Eur. J. Enterp. Technol.* **2020**, *2*, 104. [CrossRef]